BJR

https://doi.org/10.1259/bjr.20170187

Received: 14 March 2017 | Revised: 6 September 2017 | Accepted: 8 September 2017

Cite this article as:
Mendes BM, Trindade BM, Fonseca TCF, de Campos TPR. Assessment of radiation-induced secondary cancer risk in the Brazilian population from left-sided breast-3D-CRT using MCNPX. *Br J Radiol* 2017; **90**: 20170187.

FULL PAPER

Assessment of radiation-induced secondary cancer risk in the Brazilian population from left-sided breast-3D-CRT using MCNPX

[1,2]BRUNO MELO MENDES, MS, [1]BRUNO MACHADO TRINDADE, PhD, [1]TELMA CRISTINA FERREIRA FONSECA, PhD and [1]TARCISIO PASSOS RIBEIRO DE CAMPOS, PhD

[1]Programa de Ciências e Técnicas Nucleares - Departamento de Engenharia Nuclear, Universidade Federal de Minas Gerais, Belo Horizonte, Brazil
[2]Centro de Desenvolvimento da Tecnologia Nuclear (CDTN/CNEN), Seção de Dosimetria das Radiações, Belo Horizonte, Brazil

Address correspondence to: Mr Bruno Melo Mendes
E-mail: *bmm@cdtn.br*

Objective: The aim of this work was to simulate a 6MV conventional breast 3D conformational radiation therapy (3D-CRT) with physical wedges (50 Gy/25#) in the left breast, calculate the mean absorbed dose in the body organs using robust models and computational tools and estimate the secondary cancer-incidence risk to the Brazilian population.
Methods: The VW female phantom was used in the simulations. Planning target volume (PTV) was defined in the left breast. The 6MV parallel-opposed fields breast-radiotherapy (RT) protocol was simulated with MCNPx code. The absorbed doses were evaluated in all the organs. The secondary cancer-incidence risk induced by radiotherapy was calculated for different age groups according to the BEIR VII methodology.
Results: RT quality indexes indicated that the protocol was properly simulated. Significant absorbed dose values in red bone marrow, RBM (0.8 Gy) and stomach (0.6 Gy) were observed. The contralateral breast presented the highest risk of incidence of a secondary cancer followed by leukaemia, lung and stomach. The risk of a secondary cancer-incidence by breast-RT, for the Brazilian population, ranged between 2.2–1.7% and 0.6–0.4%.
Conclusion: RBM and stomach, usually not considered as OAR, presented high second cancer incidence risks of 0.5–0.3% and 0.4–0.1%, respectively. This study may be helpful for breast-RT risk/benefit assessment.
Advances in knowledge: MCNPX-dosimetry was able to provide the scatter radiation and dose for all body organs in conventional breast-RT. It was found a relevant risk up to 2.2% of induced-cancer from breast-RT, considering the whole thorax organs and Brazilian cancer-incidence.

INTRODUCTION

Radiotherapy (RT) is an important tool for breast cancer treatment.[1] A randomized clinical trial, conducted by the Early Breast Cancer Trialists' Collaborative Group, demonstrated that RT associated with breast-conserving surgery significantly decreased the local recurrence and mortality.[2] Also in this study, it was observed that RT resulted in a decreased local recurrence rate, regardless of age and tumour characteristics.[2]

However, in addition to the radiotherapy benefits in breast cancer treatment, acute and late toxic effects should also be taken into account. Contralateral breast cancer, cardiac damage, and ipsilateral lung cancer can be mentioned as late radiation-induced effects. Cardiac damage and second malignancy contribute to increased long-term mortality of the patients undergoing breast-RT.[2]

The occurrence of toxic RT late effects in organs at risk (OAR) adjacent to the planning target volume (PTV) has motivated the dosimetric analysis expansion throughout the entire body. Some authors have used the MCNP code to simulate radiotherapy procedures and calculate PTV and OAR absorbed doses.[3,4] However, only simplified computational analytical phantoms were employed in these studies. Donovan et al. [5] used the Rando phantom and thermoluminescent (TLD) dosimeters to provide experimental measurements of the mean absorbed dose and estimate the second cancer-incidence risk for different breast-RT procedures.[5] This study can be considered as a particular case of risk assessment, due to the peculiar anatomy and homogeneous composition of the solid material constituting of the Rando phantom, and the measurement positions (discrete points).

The present study aims to evaluate the dosimetry in breast-RT by two parallel-opposed fields in 6 MV, calculate the mean values of the absorbed doses for all female phantom segmented organs and estimate the secondary cancer-incidence risk induced by breast-RT using a stochastic computational code. Breast-RT protocol was simulated using the MCNPx code, and the mean absorbed doses for several organs were obtained. Lifetime Attributable Risk (LAR) was calculated for various body organs, including lung and breast, by considering different age groups of the Brazilian female population.

METHODS AND MATERIALS

The VW female phantom[6,7] was adapted for whole breast radiotherapy simulation. This voxelized phantom, based on Visible Female images,[8] was segmented with 63 different organs/tissues. This model represents a female of 165 cm of height and 98 kg weight. The voxel dimensions were adjusted to $5 \times 5 \times 5$ mm^3. The left breast was chosen for irradiation because it presents a higher risk of cardiac involvement. Figure 1 shows the VW model version used in this study.

Two parallel-opposed tangential beams with the same weight were simulated, following 3D conformational radiation therapy (3D-CRT). The software interface "posiciona_feixe_3D", of the SISCODES code, was used for positioning the two photon portals.[9] The source-isocentre distance was set to 100 cm. The photon energy spectrum was reproduced from the literature.[10] Wedge filters equivalent to W15 (15°) were added with appropriate orientation. The parallel-opposed fields received the same beam-incidence distribution, *i.e.* same weight. PTV was defined in the left breast. The reference point was placed in the centre of the left breast volume, also representing the isocentre of the two beams (Figure 1d,e), following standard RT-protocol recommendations.[11,12] The value of the absorbed dose at the reference point (RPD) was considered as 100% of the prescribed dose for normalization purpose.

MCNPx code, version 2.7.0, was used to assess the particle transport in the model.[13] The mean absorbed dose deposited on each organ per emitted photon was requested using "tally +F6". The secondary electron transport was taken into account. The absorbed dose per particle (+F6) was also requested for each voxel localized in the most irradiated region of the model. The number of photon histories accompanied by MCNPx was 5×10^7. This value was dimensioned so that the relative errors (RE) of the absorbed per voxel were sufficiently low, allowing a detailed evaluation of the VW model irradiated region.

Figure 1. Coronal (a), sagittal (b) and transverse (c) slices of VW female voxelized phantom showing the segmented organs/tissues. The reference point was identified by a circle in the left breast (d and e).

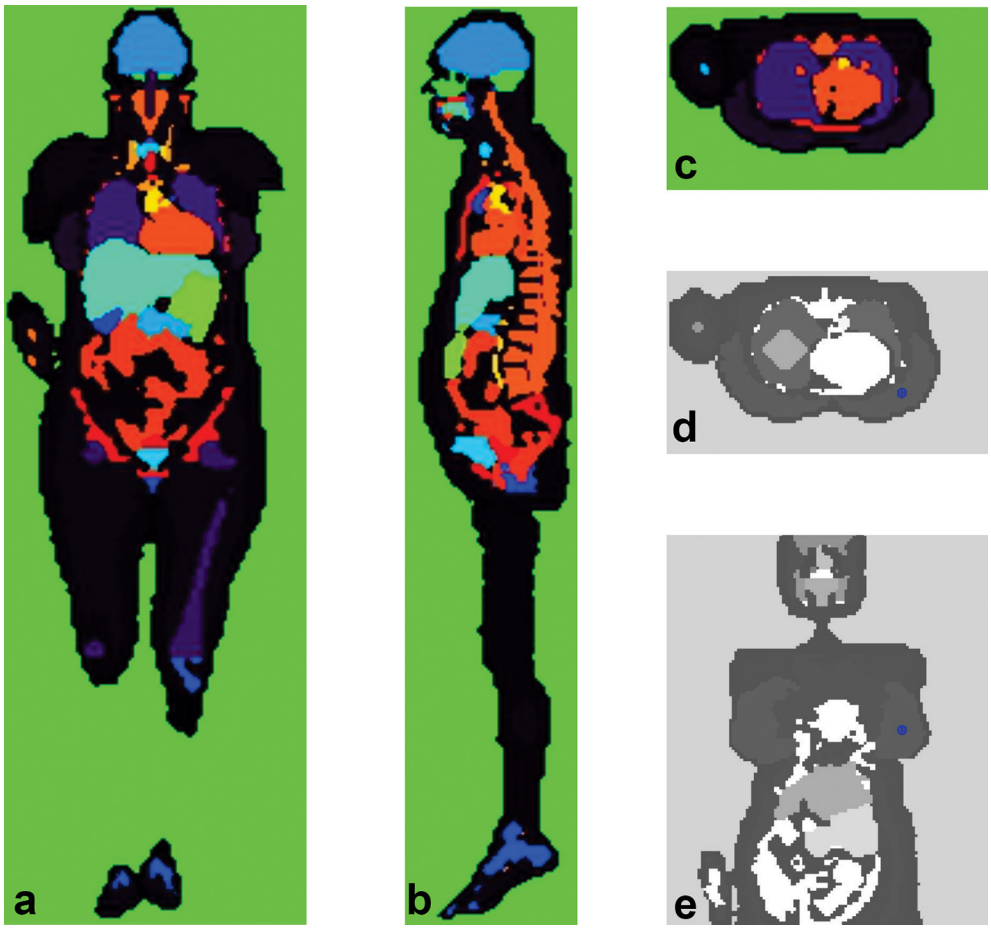

The evaluations of the mean absorbed dose at an organ (OMD) for all OARs were performed for two RPDs, as follows: (i) RPD set to 40 Gy (coil RPD_{40}) for validation of the simulations with experimental data from the literature;[5] (ii) RPD set to 50 Gy (RPD_{50}) for 3D-CRT standard Breast-RT and for BEIR VII risk evaluations.

MC simulation with RPD_{40} was performed for OMD comparison with the experimental values of Donovan et al.[5] Indeed, Donovan et al. measured the absorbed doses resulting from 3D-CRT with two tangential, wedged beams targeting the whole breast to 40 Gy in 15 fractions (40 Gy/15#).[5] Currently, in the UK, hypofractionated RT is the standard prescription.[5] A physical anthropomorphic phantom (RANDO®) and TLD were used for experimental measurement of the absorbed dose in OARs.[5] The OMD at RPD_{40} was calculated for the organs cited in the reference data.[5]

Also, RPD was set up to 50 Gy for MC simulation of standard breast-RT. Breast-3D-CRT with two parallel-opposed tangential beams typically prescribes a 50 Gy/25# treatment to the whole breast.[14] This protocol is still extensively used in Brazil and, possibly, in other low/middle income countries.[15] The effective dose was calculated based on OMDs. The methodology and the weight factors w_t presented in the ICRP 103 were applied.[16]

The LAR of a second cancer-incidence induced by breast-RT was estimated according to the methodology of BEIR VII.[17] Mean absorbed dose values in organs calculated for standard RT (50Gy/25#) were used for the estimates. Risk transport for the Brazilian population took into account the estimates of female mortality by age group provided by *Instituto Brasileiro de Geografia e Estatística* - IBGE[18] and the incidence data for different cancers in Brazilian female population by age group, adapted from a study of *Instituto Nacional do Câncer* - INCA.[19] Two methodologies were adopted for estimation of RBM mean absorbed dose for leukaemia risk calculations: (i) taking into account the mean absorbed doses in the ribs; and (ii) excluding the ribs on the calculations. Some ribs must hold large absorbed doses up to 50 Gy. The BEIR VII methodology is not applicable to these dose levels.[17] On the other hand, there must be a good mass proportion of the ribs with absorbed doses lower than 1.0 Gy. As it was not possible to include spatial dose distribuition of the ribs at the calculations but only the mean absorbed dose, the two extreme possibilities to report the leukaemia risk seems to be appropriated whose exact value is between the extremes.

An "in-house" made C^{++} program provided 3D images of the absorbed dose and RE per voxel of the VW phantom and dose/volume histograms for OARs and also calculated: (i) the dose inhomogeneity index (IHI), defined as the percentage of PTV where the absorbed dose is less than 95% or greater than 107%, being adopted RPD of 100%; (ii) the conformity index (CI) calculated as the quotient of the volumes of the PTV receiving at least RPD and of the total PTV and (iii) the homogeneity index (HI) being the maximum dose divided by the RPD.

RESULTS

Absorbed doses per voxel and quality indicators for breast-RT in VW phantom

Graphical representations of the absorbed dose per voxel are shown in Figure 2a-c. The absorbed doses were normalized by RPD per photon emitted by the source (*i.e.* 3.63E-14 Gy.fóton^{-1}), which is equivalent to 100%. The mean dose in PTV (volume = 658 cm^3) was 105% of RPD, within a 94 to 124% range.

The IHI was 24% (IHI: < 95% + > 107%). It was observed that 0.1% of the PTV was irradiated with absorbed doses lesser than 95% of RPD and 23.9% with absorbed doses greater than 107% of RPD. The CI was 0.93 and HI was 1.24 in the simulated case. In the left breast voxels, the mean RE was 2% (range: 1 – 2%),

Figure 2. Absorbed dose per voxel, normalized by RPD (100% = 3.63E-14 Gy.photon^{-1}). Coronal (a), sagittal (b) and transverse (c) slices of the VW model (RP represented as a small circle; PTV emphasized by the shaded region); and (d) the relative error per voxel in a transverse slice. PTV, planning target volume; RP, reference point; RPD, dose at the reference point.

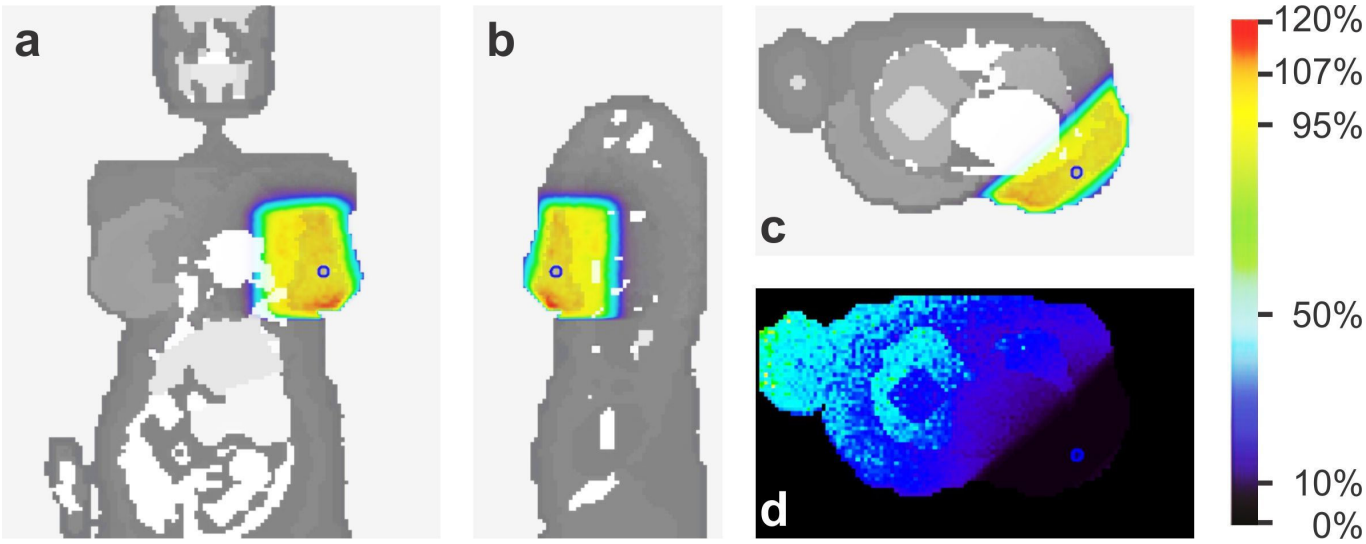

evaluated in the MCNPx. The spatial distribution of the RE is shown in Figure 2d.

Dose/volume histograms

The differential dose-volume histogram for the PTV is presented in Figure 3a. The absorbed dose normalized per RPD (below 95% or greater than 107%) occurred in 24% of PTV, confirming the calculated IHI value. It is noted that most of the inhomogeneity refers to the absorbed dose greater than 107% of RPD, which results in a high conformity index of 0.93.

The cumulative DVH for PTV is shown in Figure 3b. It can be observed that 99.9% of PTV receives more than 95% of RPD, while 93% of PTV receives 100% or more of RPD. These values meet the ICRU-50 recommendations.[14]

The cumulative dose/volume histograms for the OAR, heart and lung, are shown in Figure 3c,d, respectively. Considering an absorbed dose of 50 Gy in RPD, only 2.2% of the heart volume and 4.9% of the left-lung volume received doses greater than 30 Gy.

OMD Comparison from RPD_{40} simulation with experimental data[5]

The mean absorbed doses RE remained lower than 2% for most organs, with 5×10^7 number of photon histories. The exceptions were the ovaries (7.1%) and the uterus (3.4%). Both are small and distant from PTV (~50 cm) organs. Table 1 shows the experimental absorbed dose values reported by Donovan et al.[5] and the mean absorbed dose values of VW phantom organs considering the hypofractionated (40 Gy/15#) dose prescription, *i.e.* 40 Gy at RPD.

The highest percentage differences between the simulated and experimental values generated by Donovan et al.[5] were −63% (contralateral breast) and 370% (ipsilateral lung). Salivary glands and urinary bladder presented the smallest deviations: 11 and 15%, respectively.

OMD evaluations with RPD_{50} simulations for 3D-CRT standard Breast-RT

The mean absorbed dose at the Reference Point was set to 50 Gy (RPD_{50}) considering the 3D-CRT standard breast-RT (50 Gy/25#). Table 2 shows the mean absorbed dose values of VW phantom organs considering the standard breast-RT dose prescription. The OARs that received the highest mean absorbed doses were the ipsilateral lung (4.1 Gy) and the heart (2.9 Gy). The contralateral breast presents a mean absorbed dose of 0.3 Gy. This value is lower than 5.0 Gy, which is the contralateral breast limit-value defined by ICRU.[14] A mean absorbed dose of 1.2 Gy has been observed in the skin. Considering that most of the skin of the body was not irradiated directly by the beam, this is a high value. Several organs presented OMD in the 0.5 and 1.0 Gy range, like red bone marrow, muscle, thymus, liver and stomach. The mean absorbed PTV-dose was 52 Gy. This value is 4% higher than RPD_{50}.

Figure 3. (a) Differential DVH for PTV defined in the left breast, and cumulative DVH for: (b) PTV, (c) heart and (d) ipsilateral lung. DVH, dose volume histogram; PTV, planning target volume.

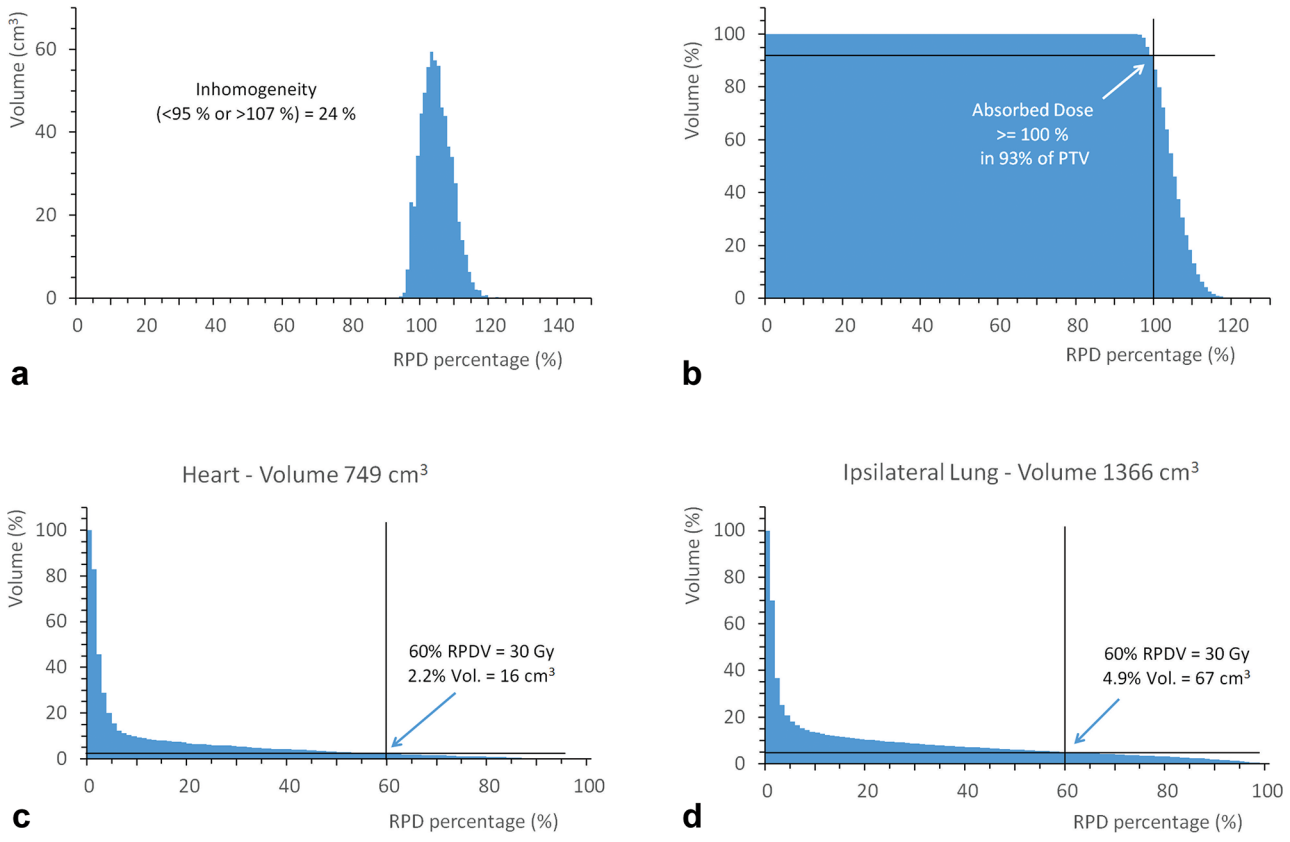

Table 1. Mean absorbed dose in VW organs for RPD_{40} and the experimental values measured in the Rando® phantom[5]

Organ or tissue	TLD—Rando[5]	MCNPx—VW[a]	
	OMD (Gy)	OMD (Gy)	SD (Gy)
Brain	0.050	0.029	0.001
Breast—contralateral	0.590	0.219	0.001
Colon	0.090	0.044	0.001
Liver	0.150	0.512	0.001
Lung—contralateral	0.110	0.178	0.001
Lung—ipsilateral	0.690	3.242	0.006
Oesophagus	0.130	0.258	0.002
Salivary glands	0.080	0.071	0.001
Stomach	0.700	0.465	0.001
Thyroid	0.100	0.160	0.002
Urinary bladder	0.020	0.017	0.001

OMD, mean absorbed dose at an organ; SD, standard deviation; TLD, thermoluminescent.
[a]Absorbed dose at the reference point of 40 Gy.

Breast-RT second cancer-incidence risk

The LAR for cancer incidence was estimated for the Brazilian population. The mean value of the organ-absorbed doses obtained through standard breast-RT simulation (50 Gy/25# - Table 2) were used for the calculations. Table 3 presents the results of LAR estimations. The range of 35 to 80 years refers to the ages at which the incidence of breast cancer is higher.[20]

The organs that presented the highest solid cancer-incidence RT-induced were the contralateral breast, the lung and the stomach. The number of lung cancer cases should be underestimated. The mean absorbed dose of ipsilateral lung was 4.0 Gy. The BEIR VII methodology is usually valid for absorbing doses lower than 1.0 Gy.[17] Thus, only the mean absorbed dose of the contralateral lung was taken into account in the estimation.

The mean absorbed dose in RBM varied considerably depending on the methodology used for its calculation. If absorbed doses in the ribs are considered, leukaemia showed the highest risk of incidence among the evaluated cancers. If not, leukaemia risks are low, and its incidence is similar to liver cancer incidence induced by breast-RT.

DISCUSSION

The IHI value obtained in this work (24%) is in the range of IHI values determined by Prabhakar et al.[21] PTVs ranging from 651 to 950 cm^3 show an IHI in the interval of 5.6 to 26.0% when a 3D-planning system was used.[21] The calculated CI (0.93) for the present simulation was better acceptable than the value obtained for the conventional RT (0.76) reproduced by Ayata et al.[22] However, the simulated breast-RT Homogeneity Index (1.24) was higher than the corresponding values (1.16) measured.[22]

Despite large differences on few organs in the Donovan measurements and simulated values, the comparison indicates a reasonable concordance between Donovan et al.[5] experimental values and these simulated values (Table 1), especially considering the material and geometric discrepancies between the phantoms. The experimental model used the Rando phantom, which consists of a homogeneous solid with 1.1 $g.cm^{-3}$ density. The mean absorbed doses were calculated from point measurements at specific positions of the phantom body. The Rando geometry has no anatomical and morphological equivalence with the VW computational phantom adopted in these simulations. The VW voxel phantom is heterogeneous, reproducing an obese female. The mean absorbed doses were obtained as the mean values calculated over the whole organs, which differ from the experimental procedure. Differences in irradiation source may also exist, but cannot be compared since essential parameters of radiation fields and spectra at Donovan et al.[5] work could not be verified.[5]

Considering the toxicity to OARs, in this case, only 16 cm^3 (2.2%) of the heart volume received doses higher than 30 Gy. Physical shield was not used on the simulations to protect OARs. However, the beam conformations were performed based on the projection of the PTV and OARs in the beam-eye views. It restricted the beam shape to the PTV boards, avoiding the OARs. The main minimum distance between heart surface and PTV was 1.8 cm. It shows equivalence to OAR and PTV distance taken in patient cases. Also, such measurements depend on the resolution of the draw of the OAR and PTV in the CT image.

Ipsilateral lung showed 4.9% of its volume (67 cm^3) with absorbed doses higher than 30 Gy. The ICRU established-limits are 30 and 200 cm^3, respectively.[14] These two values indicate that the simulated case met the ICRU-50 recommendations for OAR.[14]

The risk of incidence of a secondary cancer after the conventional breast-RT was estimated based on the Brazilian female population. The calculation of leukaemia cancer-incidence risk

Table 2. Mean absorbed dose in VW organs for RPD_{50} in 3D-CRT standard breast-RT

Organ or tissue	MCNPx – VW (RPD_{50})[a]	
	OMD (Gy)	SD (Gy)
Adrenals	0.212	0.004
Brain	0.037	0.001
Breast—contralateral	0.274	0.001
Breast—PTV	52.44	0.04
Colon	0.055	0.001
Endosteum	0.305	0.001
ET region	0.130	0.001
Gall Bladder	0.115	0.002
Heart	2.887	0.004
Kidneys	0.130	0.001
Liver	0.640	0.001
Lung—contralateral	0.223	0.001
Lung—ipsilateral	4.053	0.007
Muscle	0.736	0.0004
Oesophagus	0.323	0.002
Oral mucosa	0.112	0.001
Ovary	0.017	0.001
Pancreas	0.221	0.001
RBM	0.796	0.001
Salivary glands	0.089	0.001
Skin	1.260	0.001
Small intestine	0.074	0.001
Spleen	0.419	0.002
Stomach	0.582	0.001
Thymus	0.716	0.006
Thyroid	0.200	0.003
Urinary bladder	0.021	0.001
Uterus	0.020	0.001

CRT, conformational radiation therapy; OMD, mean absorbed dose at an organ; PTV, planning target volume; RBM, red bone marrow; RPD, dose at the reference point.
[a]Absorbed dose at the reference point of 50 Gy.

due to breast-RT was based on the RBM mean absorbed dose. The active marrow has a heterogeneous distribution in the body bones.[23] Thus, for breast-RT, there is a great heterogeneity in organ absorbed dose values. That condition is not the ideal for BEIR VII methodology.[17] When absorbed dose in the ribs was taken into account for the RBM mean dose calculation, the leukaemia cancer-incidence risk was higher than the other cancers in most age groups (0.5%–0.3% for ages 35 years and 80 years, respectively). On the other hand, if ribs absorbed doses were excluded, the risk of leukaemia induction was reduced to (0.08%–0.05% for ages 35 years and 80 years, respectively).

Some publications have reported cases of leukaemia induced by breast-RT.[2,24,25] The standardized incidence ratio reported for leukaemia incidence after breast-RT were: (i) 1.71 (SE = 0.36);[2] (ii) 1.6 [95% CI (1.2–2.1)] for ≤ 45 years female, 1.5 [95% CI (1.2–1.8)] for 46–55 years female and 1.4 [95% (CI 1.2–1.6)] for ≥ 56 years female[24] and (iii) 1.8 [95% CI (1.2–2.8)].[25] The standardized incidence ratio is the ratio between the total number of events in the cohort and the total number of expected events. An early review paper also associated breast-RT and leukaemia.[26] The real value of radiation-induced leukaemia should be between the estimated values. However, since leukemia was not reported as a major problem in breast-RT, lower incidence rates should be more probable.

The stomach, as the RBM, is also not considered an OAR.[14] However, the risk of a secondary cancer-incidence in this organ due to breast-RT ranged from 0.4 to 0.1%. Studies have reported an increase in stomach cancer incidence after the breast cancer treatment.[24,27–30] However, only the work of Mellemkjær et al.[24] has demonstrated an increase in the incidence of stomach cancer related to breast-RT. It seems curious that only Mellemkjær et al.[24] reported this association. The stomach is a radiosensitive organ[17] and relatively high absorbed doses from scattered radiation were observed in our study (0.58 Gy). Donovan et al.[5] measured experimentally (with TLD and RANDO) a mean absorbed dose in the stomach of 0.70 Gy. The relatively low baseline of breast cancer incidence in Caucasian populations[17] may complicate the association between increased incidence of stomach cancer and breast-RT. Thus, statistically significant increases could be observed only within very large cohorts. Studies with populations with a higher baseline incidence of stomach cancer might help to solve this issue.

The summation of the secondary cancer-incidence risk for breast-RT estimated in this work was in the range of 2.2–1.7% and 0.6–0.4% for the ages of 35 years and 80 years, respectively. According to a previous UK population study, the risk of cancer induction due to breast-RT was 1.1 to 0.1%[5]. However, in Donovan et al.[5] work, the leukaemia and the group "Other Solid Cancers" were not considered.[5] In addition, the PTV prescribed dose was 20% lower (40 Gy).

It can be stated that the secondary cancer-incidence risk for breast-RT is low compared to its benefits, which indicates a local control of the breast tumour. However, it should be kept in mind that LAR values were obtained from a computational model that represents a specific individual. In addition, the uncertainties involved in LAR calculations are usually about a factor of two.[31] In this analysis, we did not include the occurrence of radiation-induced Sarcomas in the breast-RT, which should add a 0.2% cancer incidence to the previously mentioned values.[1] It is considered that 10 Gy is the minimum dose for induction of this type of cancer;[32] therefore, irradiated breast has high cancer-incidence risk. Such an absorbed dose value is outside the BEIR VII range (< 1 Gy)[17] and therefore outside the scope of this study. Similarly, the risk of radiation-induced cancer was not calculated for organs with mean doses greater than 1.0 Gy - irradiated breast, ipsilateral lung and heart.

Table 3. Lifetime attributable risk of cancer incidence calculated for the Brazilian population considering RPD_{50}

LAR (cancer incidence per 100,000 treated females)							
Organs	OMD (Gy)	Age of treatment (years)					
		35	40	50	60	70	80
Stomach	0.582	392	380	344	289	210	111
Colon	0.055	28	27	25	21	15	7
Liver	0.640	87	85	80	68	49	26
Lung (contralateral)[a]	0.223	384	380	361	316	240	140
Breast (contralateral)	0.274	548	406	205	93	37	11
Uterus	0.020	4	4	3	2	1	0
Ovary	0.017	4	4	3	3	1	1
Urinary bladder	0.021	11	11	10	9	7	4
Other solid cancers[b]	0.055	117	110	92	69	44	20
Thyroid	0.200	79	47	14	4	1	0
All solid cancers	–	1654	1454	1138	873	606	321
Leukemia_1[c]	0.796	510	509	501	480	425	322
Leukemia_2[d]	0.122	81	81	80	77	68	53

LAR, lifetime attributable risk; OMD, mean absorbed dose at organ.
[a]Ipsilateral lung has mean absorbed dose out of BEIR VII range (> 1.0 Gy).
[b]Colon mean absorbed dose, according to BEIR VII methodology.
[c]Mean absorbed dose in RBM.
[d]Mean absorbed dose in RBM excluding absorbed doses in the ribs.

The introduction of new breast-RT techniques has shown good results with regard to dose uniformity and PTV coverage.[22,33] However, these new technologies are increasing the healthy tissue mean absorbed dose and the whole body irradiation.[5,22,33,34] Care should be taken so that the local control benefit is not supplanted by an increase in the secondary cancer-incidence.

Radiation therapy is an elaborate science. Breast-RT can be provided by various megavoltage (MV) LINAC teletherapy protocols such as 3D-CRT with physical wedge, 3D-CRT with virtual wedge realized by a moving collimator jaw, 3D-CRT with field-in-field, Breast Intense Modulate RT (IMRT) with multileaf or tomotherapy[11] and among others RT modalities as electrons teletherapy or brachytherapy. A possible difference in such MV protocols is the static or dynamic methods of shaping the fields. There is a diversity of applying physical parameters such as beam´s numbers, beam position and orientation, spectra, weighting the monitor units (MU), diversities of the regular field size, number of segmentations of each field, regular or irregular shape beams or a fan-shape beams, in addition to the presence of field modulators such as custom Cerrobend blocking, physical wedges, compensators, bolus, static or dynamic multileaf or independently movable jaws (virtual wedges). Each method has a promise of improving the spatial dose distribution in the PTV and sparing the deleterious effects on the OAR and in the skin.[35] Better esthetic results, better dose distribution in PTV and lower collateral effects are the breast-RTs promises.[11] The MCNP simulation in 3D-CRT with physical wedge has been addressed here; however, the full commitment to other modalities will be considered in the near future and each modality may provide its own scattering radiation profile and thus a mean absorbed dose at organs.

Radiation therapy centres have been improving breast-RT by applying new techniques when available. Although dynamic virtual-wedges reduced the scatter-radiation outside-field and 3D-CRT with physical-wedges may not represent the state-of-art in breast-RT, physical-wedges continue to be used in RT in a large number of developing countries in which new technologies are not available. Therefore, the present studies in the risk of secondary radiation-induced cancer in conventional 6 MV two-oppose fields breast-RT with physical-wedges based on MCNP-simulations were the start for improving knowledge on the theme.

A set of specific therapy planning system (TPS) predicts the absorbed dose dedicated to each RT-protocol. In the TPS, specific problems are addressed such as IMRT protocol in which an inverse spatial-dose problem is applied to generate an ideal spatial-dose distribution.[36] Inspite of that inter and intra leaf transmissions, non-divergent leaf end design and leaf scatter are present. Thus, groove leakage is present in IMRT. It is already known that low dose regions receive substantially more radiation than simulated in an ideal multileaf collimator.[37] TPS shall predict all leakage and radiation transmitting from gantry; however, it may not fulfil in the present TPS.[38] The studies in risk of secondary radiation-induced cancer in the breast-RT based on IMRT shall consider all radiation components generated on the

gantry and the possible inverse dosimetric problem applied. It is a complex problem to start simulating IMRT on MCNP code.[39] However, the work of Fonseca and Campos[39] is limited to situations in which the inverse problem was not applied. The evaluation of the risk of secondary radiation-induced cancer based on MCNP is possible only after IMRT-MCNP simulations are fully implemented.

The Monte Carlo technique (MC) for RT-dose prediction in heterogeneous medium has already been proposed based on MCNP, EGS or GEANT codes, among others.[40,41] Although the full MC-method has not yet been implemented in clinical RT, TPSs based on MC have lately been introduced into clinical practice. Indeed, Monaco TPS provides the MC and Collapsed Cone algorithms coupling.[42] Monaco addressed MC in Kernel evaluation; however, the Therma method of calculation remained. Therefore, Monaco may not be considered as a full implementation of MC for clinical applications. Further studies are required to have the full MC running in clinical RT.

The state-of-phase´s type-source defined by some MC codes (MCNP and EGS) can be useful in simulating static-field modulators established in RT-machines. In each situation, reliable reproductions of the beam-output and the scatter-radiations (from the different radiation components) are two requirements for achieving an accurate simulation. In the present 3D-CRT breast-RT with physical wedges simulations, these requirements were previously fulfilled through the examination of the output beam parameters and the dose-flatness at 10 cm depth in water for a 10 × 10 window and 6 MV beam. In addition, RT quality indicators (HI, CI, IHI and doses in OARs and PTV) of the present simulations were found adequate, taking into account the ICRU-50 recommendations.[14] As shown, those parameters reproduce similar values found in clinical situations. In addition, intercomparison of a 40 Gy breast-RT phantom experimental dosimetry[5] and our data was performed for helping validation. In such condition, outside-field absorbed-doses were evaluated with some confidence. Thus, average-organ-dose and equivalent-dose could be estimated, and radio-induced cancer-incident risk was predicted to a specific population. Any other RT-protocol simulated on MCNP must perform similar data validation, for which experimental data may not be easily reproduced or found in the literature.

The simulation of time-dependent state-of-phase type-source in MCNP code has still been a challenge. The reliable simulations of moving wedges by dynamic jaw or dynamic multileafs with accuracy in beam-output and scatter-radiation reproduction has not been performed previously. Although outside-field dose -predictions by direct measurements in patients or TPSs have already been presented in literature for various breast-RT cases including IMRT and 3D-CRT with static and dynamic wedges,[36] their reliable reproductions in MC simulations are still in progress. Actually, these are not reliable in evaluating organ-dose far from isocentre based on MC using dynamic time-dependent sources. Improvements in source definition, including time-dependent intensity, will be needed. At the present time, static wedges were used in 3D-CRT simulations. Further investigation will be required to establish at a time-dependent RT-source in MCNP.

Computational simulation of breast-RT using stochastic codes can generate a wide range of information with good correlation with experimental data. However, computational time is high (~120 h), even using a 120-cores cluster. Thus, interactive adjustments in beam positioning, size, filtration and the proportional intensity becomes impracticable for the stage of the software developed.

Future efforts will be focused on the adaptation of ICRP female adult referenced phantom[23] for breast-RT simulations and on the improvements in MCNPx breast-RT planning tools.

CONCLUSIONS

The RT quality indicators (HI, CI, IHI and doses in OARs and PTV) of the present simulations indicate that the beam positioning, the source definition and the other computational parameters were established adequately by taking into account the ICRU-50 recommendations.[14]

Considering the results of this study, it can be stated that some organs that normally are not considered as OARs presented relatively high mean absorbed doses. Among these, the most significant are red bone marrow (0.8 Gy) and stomach (0.6 Gy). The estimated stomach cancer-incidence risk was high (0.4%, –35 years to 0.1%, 80 years for the Brazilian population). Leukaemia estimated incidence risk varied in a wide range, but is not negligible. Thus, it is suggested that even if they are not traditionally considered OARs, particular attention should be given to them during breast-RT planning.

The total secondary cancer-incidence risk due to breast-RT, for the Brazilian population, was considered high (2.2–1.7% and 0.6–0.4%); however, when the local control benefit is taken into account such values are acceptable. Although uncertainties associated with risk assessment are high, cancer-incidence risk studies may be useful for assessing breast-RT risk/benefit ratio, especially when new radiotherapy techniques are planned to be introduced in clinical practice.

In the case under study, contralateral breast, contralateral lung, stomach cancers and possible leukaemia presented the higher cancer-incidence risk for breast-RT. Care should be taken to avoid the increase of absorbed dose in these organs, either in the treatment planning or in the development of new breast-RT techniques, in order to minimize a secondary cancer-incidence risk.

Methodologies for secondary cancer-incidence risk estimation for organs with an average dose higher than that recommended by the BEIR VII (> 1.0 Gy) should be developed to improve the accuracy of the data generated in this study, especially with respect to irradiated breast, ipsilateral lung, heart and ribs.

ACKNOWLEDGMENTS

We would like to thank the *Laboratório de Metrologia de Nêutrons of the Instituto de Radioproteção e Dosimetria* (IRD/

CNEN) for consenting the use of high-performance cluster for the calculations. The authors are thankful to Conselho Nacional de Desenvolvimento Científico e Tecnológico (CNPq-RE-BRAT-SUS).

REFERENCES

1. Cancer.gov. NCI. Breast Cancer Treatment (PDQ®) Health Professional Version. National Cancer Institute (US). [Updated February 2017; cited March. 2017]. Available from: https://www.cancer.gov/types/breast/hp/breast-treatment-pdq.
2. Clarke M, Collins R, Darby S, Davies C, Elphinstone P, Evans V, et al. Early breast cancer trialists' collaborative group (EBCTCG). Effects of radiotherapy and of differences in the extent of surgery for early breast cancer on local recurrence and 15-year survival: an overview of the randomised trials. *Lancet* 2005; **366**: 2087–106.
3. Pignol JP, Keller BM, Ravi A. Doses to internal organs for various breast radiation techniques-implications on the risk of secondary cancers and cardiomyopathy. *Radiat Oncol* 2011; **6**: 5–6. doi: https://doi.org/10.1186/1748-717X-6-5
4. Berris T, Mazonakis M, Stratakis J, Tzedakis A, Fasoulaki A, Damilakis J. Calculation of organ doses from breast cancer radiotherapy: a Monte Carlo study. *J Appl Clin Med Phys* 2013; **14**: 133–46. doi: https://doi.org/10.1120/jacmp.v14i1.4029
5. Donovan EM, James H, Bonora M, Yarnold JR, Evans PM. Second cancer incidence risk estimates using BEIR VII models for standard and complex external beam radiotherapy for early breast cancer. *Med Phys* 2012; **39**: 5814–24. doi: https://doi.org/10.1118/1.4748332
6. Mendes BM, Almeida IG, Trindade BM, Campos TPR. A female voxel phantom for radiopharmaceuticals internal dosimetry. In: *4th international nuclear chemistry congress*. Maresias, Brasil: 2014. 317. 317–8.
7. Mendes BM, Fonseca TCF, Almeida IG, Trindade BM, Campos TPR. MCNPx Computational Estimation of the Calibration Factor of an In Vivo Counter for ^{18}F-FDG Activity Incorporated in the Brain. In: *XVI International symposium on solid state dosimetry - ISSD 2016*. Tuxtla Gutiérrez, México; 2016. pp. 6–22.
8. NLM. [homepage on the internet]. National Library of Medicine - The Visible Human Project. 2017. Available from: https://www.nlm.nih.gov/research/visible/visible_human.html [Updated 2015 Sep; cited 2016 Mar]
9. Trindade BM, Campos TPRde. Sistema computacional para dosimetria de nêutrons e fótons baseado em métodos estocásticos aplicado a radioterapia e radiologia. *Radiol Bras* 2011; **44**: 109–16. doi: https://doi.org/10.1590/S0100-39842011000200011
10. Mesbahi A, Mehnati P, Keshtkar A. A comparative Monte Carlo study on 6MV photon beam characteristics of Varian 21EX and Elekta SL-25 linacs. Iran. *J. Radiat. Res* 2007; **5**: 23–30.
11. Perez CA, Brady LW. *Principles and practice of Radiation Oncology*. Philadelphia, USA: Lippincott-Raven Publishers; 2003.
12. Bellon JR, Wong JS, MacDonald SM, Ho AY. *Radiation therapy techniques and treatment planning for breast cancer (practical guides in Radiation Oncology*. New York, USA: Springer International Publishing; 2016.
13. Pelowitz DB (ed.). "MCNPX Users Manual Version 2.7.0" Report No: LA-CP-11-00438. 2011.
14. International Commission on Radiation Units and Measurements. Prescribing, recording, and reporting photon beam therapy ICRU Report 50. Bethesda, USA: International Commission on Radiation Units and Measurements. 1993.
15. Marta GN, Hanna SA, Martella E, Silva JL, Carvalho HA. Early stage breast cancer and radiotherapy: update. *Rev Assoc Med Bras* 20112011; **57**: 459–64; **57**: 459–64. doi: https://doi.org/10.1016/S0104-4230(11)70095-1
16. ICRP Publication 103. 2007 Recommendations of the International Commission on Radiological Protection. *Ann ICRP* 2007; **37**: 1–332.
17. NRC. *National research council of the national academies. Health risks from exposure to low levels of ionizing radiation: BEIR VII phase 2*. Washington DC, USA: National Academies Press; 2006.
18. IBGE. *Instituto Brasileiro de Geografia e Estatística - Tábua completa de mortalidade para o Brasil – 2014 – Breve análise da evolução da mortalidade no Brasil*. Rio de Janeiro, Brasil: IBGE; 2015.
19. INCA. *National Cancer Institute José Alencar Gomes da Silva (INCA) - Cancer in Brazil: data from the population-based registries, Volume 4*. Rio de Janeiro, Brasil: INCA; 2013.
20. INCA. *Instituto Nacional do Cancer José Alencar Gomes da Silva (INCA). Estimativa 2016: incidência de câncer no Brasil*. Rio de Janeiro, Brasil: INCA; 2015.
21. Prabhakar R, Rath GK, Julka PK, Ganesh T, Joshi RC, Manoharan N. Breast dose heterogeneity in CT-based radiotherapy treatment planning. *J Med Phys* 2008; **33**: 43–8. doi: https://doi.org/10.4103/0971-6203.41191
22. Ayata HB, Güden M, Ceylan C, Kücük N, Engin K. Comparison of dose distributions and organs at risk (OAR) doses in conventional tangential technique (CTT) and IMRT plans with different numbers of beam in left-sided breast cancer. *Rep Pract Oncol Radiother* 2011; **16**: 95–102. doi: https://doi.org/10.1016/j.rpor.2011.02.001
23. ICRP. Adult reference computational phantoms. *Ann ICRP* 2009; **39**: 1–166.
24. Mellemkjaer L, Friis S, Olsen JH, Scélo G, Hemminki K, Tracey E, et al. Risk of second cancer among women with breast cancer. *Int J Cancer* 2006; **118**: 2285–92. doi: https://doi.org/10.1002/ijc.21651
25. G-P Y, Schantz SP, Neugut A I, Zhang Z-F. Incidences and trends of second cancers in female breast cancer patients: a fixed inception cohort-based analysis (United States. *Cancer Cause Control* 2006; **17**: 411–20.
26. Marcu LG, Santos A, Bezak E. Risk of second primary cancer after breast cancer treatment. *Eur J Cancer Care* 2014; **23**: 51–64. doi: https://doi.org/10.1111/ecc.12109
27. Schaapveld M, Visser O, Louwman MJ, de Vries EG, Willemse PH, Otter R, et al. Risk of new primary nonbreast cancers after breast cancer treatment: a dutch population-based study. *J Clin Oncol* 2008; **26**: 1239–46. doi: https://doi.org/10.1200/JCO.2007.11.9081
28. Evans HS, Lewis CM, Robinson D, Bell CM, Møller H, Hodgson SV. Incidence of multiple primary cancers in a cohort of women diagnosed with breast cancer in southeast England. *Br J Cancer* 2001; **84**: 435–40. doi: https://doi.org/10.1054/bjoc.2000.1603
29. Adami HO, Bergkvist L, Krusemo U, Persson I. Breast cancer as a risk factor for other primary malignant diseases. A nationwide cohort study. *J Natl Cancer Inst* 1984; **73**: 1049–55.
30. Murakami R, Hiyama T, Hanai A, Fujimoto I. Second primary cancers following female breast cancer in Osaka, Japana population-based cohort study. *Jpn J Clin Oncol* 1987; **17**: 293–302.

31. O'Connor MK, Li H, Rhodes DJ, Hruska CB, Clancy CB, Vetter RJ. Comparison of radiation exposure and associated radiation-induced cancer risks from mammography and molecular imaging of the breast. *Med Phys* 2010; **37**: 6187–98. doi: https://doi.org/10.1118/1.3512759
32. Sheth GR, Cranmer LD, Smith BD, Grasso-Lebeau L, Lang JE. Radiation-induced sarcoma of the breast: a systematic review. *Oncologist* 2012; **17**: 405–18. doi: https://doi.org/10.1634/theoncologist.2011-0282
33. Borges C, Cunha G, Teixeira N. Comparação de diferentes técnicas de irradiação de mama em radioterapia com recurso a acelerador linear em modo de fotões. *Saúde & Tecnologia* 2013; **9**: 33–9.
34. Donovan EM, Ciurlionis L, Fairfoul J, James H, Mayles H, Manktelow S, et al. Planning with intensity-modulated radiotherapy and tomotherapy to modulate dose across breast to reflect recurrence risk (IMPORT High trial). *Int J Radiat Oncol Biol Phys* 2011; **79**: 1064–72. doi: https://doi.org/10.1016/j.ijrobp.2009.12.052
35. Javedan K, Zhang GG, Hoffe S, Feygelman V, Forster K. Comparing dose in the build-up region between compensator- and MLC-based IMRT. *J Appl Clin Med Phys* 2012; **13**: 1–12. doi: https://doi.org/10.1120/jacmp.v13i5.3748
36. Chen WZ, Xiao Y, Li J. Impact of dose calculation algorithm on radiation therapy. *World J Radiol* 2014; **6**: 874–80. doi: https://doi.org/10.4329/wjr.v6.i11.874
37. Popple RA, Fiveash JB, Brezovich IA. Effect of beam number on organ-at-risk sparing in dynamic multileaf collimator delivery of intensity modulated radiation therapy. *Med Phys* 2007; **34**: 3752–9. doi: https://doi.org/10.1118/1.2779862
38. Muralidhar KR, Murthy PN, Sresty NV, Dixit PK, Kumar R, Raju AK. Measurement of back-scattered radiation from micro multileaf collimator into the beam monitor chamber from a dual energy linear accelerator. *J Med Phys* 2007; **32**: 65–7. doi: https://doi.org/10.4103/0971-6203.33243
39. Fonseca TC, Campos TP. SOFT-RT: Software for IMRT simulations based on MCNPx code. *Appl Radiat Isot* 2016; **117**: 111–7. doi: https://doi.org/10.1016/j.apradiso.2015.12.061
40. Juste B, Miro R, Gallardo S, Verdu G, Santos A. Considerations of MCNP Monte Carlo code to be used as a radiotherapy treatment planning tool. *Conf Proc IEEE Eng Med Biol Soc* 2005; **3**: 2828–31. doi: https://doi.org/10.1109/IEMBS.2005.1617062
41. Randeniya SD, Taddei PJ, Newhauser WD, Yepes P. Intercomparision of Monte Carlo radiation transport codes MCNPX, GEANT4, and FLUKA for simulating proton radiotherapy of the Eye. *Nucl Technol* 2009; **168**: 810–4. doi: https://doi.org/10.13182/NT09-A9310
42. Barbeiro AR, Ureba A, Baeza JA, Linares R, Perucha M, Jiménez-Ortega E, et al. 3D VMAT verification based on monte carlo log file simulation with experimental feedback from film dosimetry. *PLoS One* 2016; **11**: e0166767–19. doi: https://doi.org/10.1371/journal.pone.0166767